LUNAR ELEMENTAL ABUNDANCES FROM CHANDRAYAAN-2 LARGE AREA SOFT X-RAY SPECTROMETER (CLASS): S. Narendranath[1], Koushal Vadodariya[1], Netra S Pillai[1], Radhakrishna V[1], Anurag Tyagi[1], Santosh Vadawale[2], Mithun N P S[2], Shanmugam M[2], Arpit Patel[2], Srikar P Tadepalli[1], Reena Yadav[1], Brajpal Singh[1], Vaishali S[1], P. Sreekumar[3], Megha Bhatt[2], Neeraj Satya[1], Akash Shetty[1], H.N. Suresha Kumar[1], G Balaji[1], Kumar[1], Venkata Raghavendra[1], Anil Agarwal[1], kcshyama@ursc.gov.in, [1]U R Rao Satellite Centre, ISRO, Bengaluru, [2] Physical Research Laboratory, [3]Space Science Office, ISRO HQ.

Introduction: Solar X-rays trigger X-ray fluorescence (XRF) lines from the lunar surface providing direct evidence for identification of the major elements from airless bodies. C1XS [1] on Chandrayaan-1 using the technique provided elemental maps [2] of 50km to several hundred kilometers for a few regions of the Moon. CLASS [3] is similar in design but with four times the geometric area of C1XS and operating in the 0.5 to 20 keV energy range. From the 100 km polar orbit the instantaneous ground pixel is 12.5 km x 12.5 km. An Solar X-ray Monitor (XSM) [4] simultaneously measures the varying solar X-ray spectrum in the 1- 15 keV energy range which is a crucial input for determining the elemental abundances from the lunar surface.

We present the first results derived from CLASS covering the nearside equatorial (11.5 N, 36W) to the northern high latitudes (72.9N, 35.5W), one of the most complex areas on the Moon encompassing a variety of geochemical settings. Figure 1 shows the track on 18th November 2019 12:55:36 UT to 13:15:28 UT during which there was an enhancement in solar flux triggering XRF from lunar surface. We have divided the CLASS foot prints into six sections as marked in Figure 1. They pass through (1) ray systems of craters Copernicus, Kepler and Arisstrahus (2) Mare imbrium (3) Sinus Iridium (4) Northern Imbrium Noritic regions (5) Mare Friogoris (6) Highland.

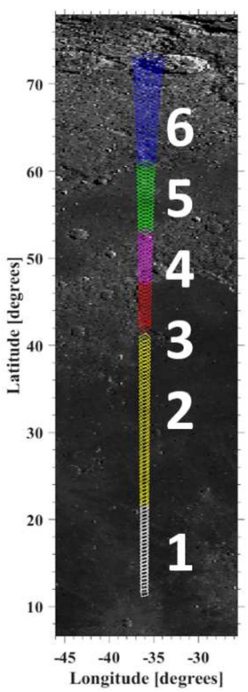

Figure 1: Track during the observation

Analysis: CLASS carried sixteen radioactive sources for onboard calibration from which the calibration parameters derived on ground could be verified. There is a continuum background resulting from particles in the ambient environment which changes significantly in flux as well as spectral shape during geotail crossings. For the data set here, we chose a night side observation when there are no geotail related enhancements.

Solar spectral analysis: The incident solar spectrum is one of the most important inputs to convert the observed lunar XRF line flux to weight percent (wt) %. In addition, scattered lines from the Sun contribute to the observed lunar X-ray spectrum which also has to be modeled. We model the solar spectrum measured by XSM (Figure 2) using the *vapec* model in XSPEC. The sun was not in the field of view of XSM from 12:55: 13:05:04 (pixel 1 and 2 in figure 1). Hence we use the solar spectrum for the time of observation of pixel 3 for pixel 1 and 2 as well.

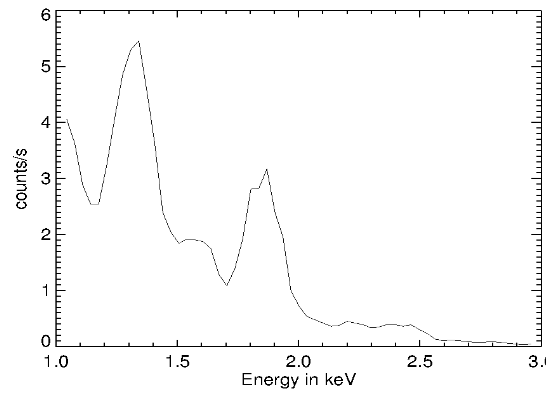

Figure 2: Solar spectrum measured by XSM during observations of pixel 3 (18 Nov 2019). Emission lines from the flare plasma can be clearly seen.

XRF lines observed with CLASS. CLASS detected the XRF lines from O, Mg, Al and Si in all six pixels during this observation. In addition, an Fe-L line (at 0.72 keV) in pixel 1 and 2 and a Na- Kα line (at 1.01 keV) in pixel 1 is also observed. Oxygen line flux is the highest with which elemental maps at ~12 km would be possible. Figure 3 shows the lunar X –ray spectrum in this track for a 25 km x 25 km pixel from region 2 where there is a clear detection of four XRF lines corresponding to O, Mg, Al and Si. However, we derived abundances for the six ground pixels defined earlier for better statistics.

Spectral analysis: The back ground subtracted CLASS X-ray spectra are modeled in XSPEC using a Gaussian function for the XRF lines (Figure 4). The scattered solar spectrum from the lunar surface is calculated with an average assumed composition for the region of observation (Mare or highland) and included as a model component. The scattered lines from Sun are clearly seen in the observed lunar spectrum which aids in modeling this fraction accurately (Figure 5). From the best fit parameter values, the XRF line flux is derived along with uncertainties.

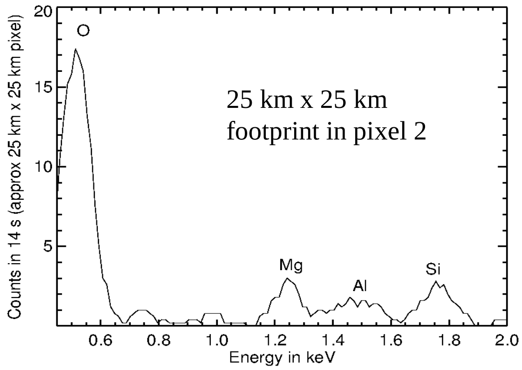

Figure 3: XRF lines of O, Mg, Al and Si detected from a ground pixel of 25 km x 25 km in the imbrium basin

Abundances: We use an algorithm named *'x2abund'* [5, 6] for estimating the wt% from X ray line flux. The solar spectrum from XSM is used as the input and from a matrix of wt% values for all major elements, XRF line flux is calculated using a fundamental parameter method. The calculated flux is then compared to the observed and best fit values are derived using a chi-square minimization algorithm. The algorithm has been verified extensively using laboratory experiments and was developed for analysis of similar data from C1XS [7, 8] on Chandrayaan-1.

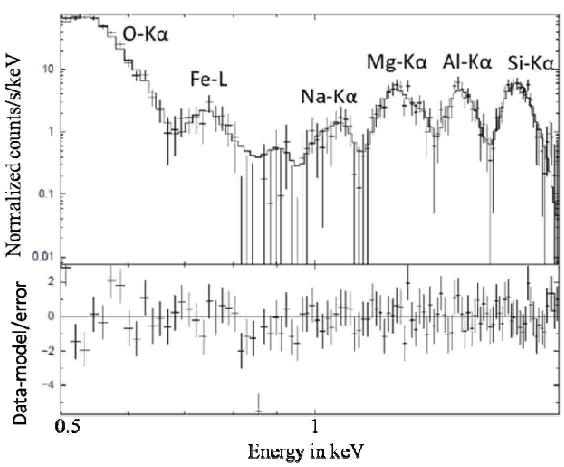

Figure 4: Lunar X-ray spectra in the imbrium basin region (pixel 2) fitted with a model with lines and scattered continuum.

CLASS due to the low solar activity. These values are necessary to generate the matrix of compositions with wt% of all major elements. We have used Ca, Ti and Fe wt% values from LP-GRS [9] in this work. The abundances derived from the six regions are plotted in figure 6 along with values from LP-GRS, Apollo soils, meteoritic samples and from APXS [10] on Chang'e-3

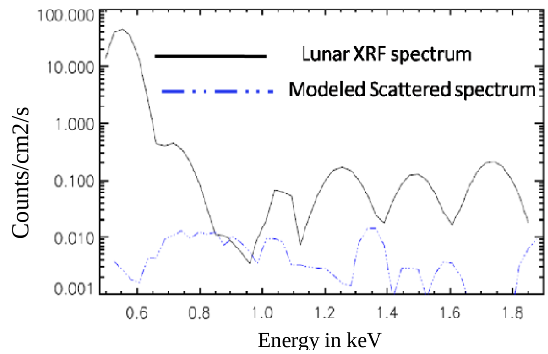

Figure 5: Lunar X-ray spectrum along with the scattered fraction of the solar spectrum.

at four locations in the imbrium basin region. CLASS values follow the general trend observed in Mare-highlands.

Summary: CLASS along with solar spectrum from XSM will enable elemental mapping at the highest resolution ever achieved. The sensitivity enables measurement of O during non-solar flare periods and of Mg, Al, and Si for A- B class solar flares.

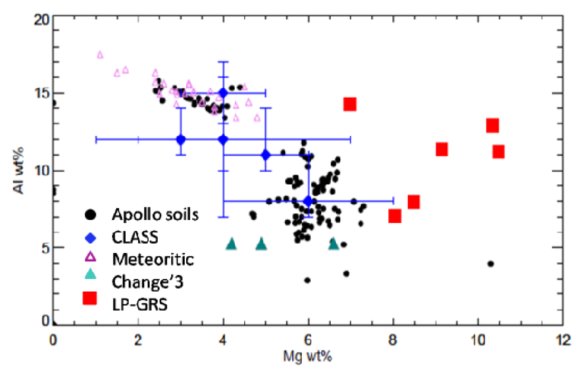

Figure 6: Abundances derived from CLASS pixels shown in blue compared to earlier investigations

Acknowledgements: We thank Usha Pandey and team at BARC, A Holland, M. Soman, J Gow (now at UCL) and P. Smith at OU, UK and to C J Howe at RAL, UK, Sreekantha C V of URSC and P S Athiray at MSFC. Our sincere appreciation to the mission, ground segment and the Chandrayaan-2 project team.

References: [1] Grande et al, *PSS* (2009), 57, 717. [2] S. Narendranath and Netra S Pillai, *50th LPSC abs.* 2516.[3] Radhakrishna et al, 42nd *LPSC abs.*1708 [4] Shanmugham et al (2019) arXiv.1910.09231. [5] Athiray et al (2013) *PSS*, *75*, 188, [6] Athiray et al (2013), *PSS*, *89*, 183 [7] Narendranath et al (2011) *Icarus*, *214*, 53. [8] Athiray et al (2014), *PSS*, *104*, 279. [9] Prettyman et al (2006) *JGR*, 111, E12007. [10] Ling et al, (2015) *Nature communication*, 6, 888.